

Polynomially restricted operator growth in dynamically integrable models

Igor Ermakov,^{1,2} Tim Byrnes,^{3,4,5,6,*} and Oleg Lychkovskiy^{7,1,2,†}

¹Russian Quantum Center, Skolkovo, Moscow 121205, Russia

²Department of Mathematical Methods for Quantum Technologies,

Steklov Mathematical Institute of Russian Academy of Sciences, 8 Gubkina St., Moscow 119991, Russia.

³New York University Shanghai, NYU-ECNU Institute of Physics at NYU Shanghai,

Shanghai Frontiers Science Center of Artificial Intelligence and Deep Learning,

567 West Yangsi Road, Shanghai, 200126, China.

⁴State Key Laboratory of Precision Spectroscopy, School of Physical and Material Sciences,

East China Normal University, Shanghai 200062, China

⁵Center for Quantum and Topological Systems (CQTS),

NYUAD Research Institute, New York University Abu Dhabi, UAE.

⁶Department of Physics, New York University, New York, NY 10003, USA

⁷Skolkovo Institute of Science and Technology, Bolshoy Boulevard 30, bld. 1, Moscow 121205, Russia.

(Dated: June 21, 2024)

We provide a framework to determine the upper bound to the complexity of a computing a given observable with respect to a Hamiltonian. By considering the Heisenberg evolution of the observable, we show that each Hamiltonian defines an equivalence relation, causing the operator space to be partitioned into equivalence classes. Any operator within a specific class never leaves its equivalence class during the evolution. We provide a method to determine the dimension of the equivalence classes and evaluate it for various models, such as the XY chain and Kitaev model on trees. Our findings reveal that the complexity of operator evolution in the XY model grows from the edge to the bulk, which is physically manifested as suppressed relaxation of qubits near the boundary. Our methods are used to reveal several new cases of simulable quantum dynamics, including a XY - ZZ model which cannot be reduced to free fermions.

Introduction Solving time dynamics of quantum many-body problems is typically an extremely difficult task. In a brute force computation of such systems, one requires solving a coupled differential equations with an exponential number of parameters with respect to the system size. In the Heisenberg formulation, an initially local observable evolves into an exponentially complex sum of non-local operators [1–6]. This proliferation of operators in the Heisenberg picture, called operator growth, has been explored recently in numerous closed [1, 2, 4, 6–11] and open quantum systems [12–18]. Understanding operator complexity is crucial for determining the boundary between solvable and unsolvable problems in quantum dynamics, distinguishing between reachable and non-reachable quantum states, and understanding how information propagates through quantum systems. In a quantum computing context, the simulability of quantum circuits is a crucial question in the context of quantum advantage and other applications [19–25].

In some special cases, the space where the operator evolution occurs may not necessarily cover the full operator space. For instance, in free-fermionic spin chains, the z -spin projection operator under Heisenberg evolution only scales polynomially with the system size [26, 27]. This restricted evolution explains the solvability of various dynamic [28–40] and transport [41–45] problems, as well as the classical simulability of matchgate circuits [26, 27, 46–48]. Moreover, different local operators within the same system can evolve in non-overlapping subspaces with varying dimensions and growth patterns. Exam-

ples include the z - and x -spin projections in the XX model [2], or edge modes decoupled from the bulk [49–52] discovered in various models. The dimensionality of this subspace, which we call the Operator Evolution Dimension (OED), provides a natural upper bound for the complexity of simulating the corresponding quantum dynamics problem.

In this paper, we introduce a framework to classify the OEDs of different local operators, which allows for a powerful way of understanding of the difference between simulable and non-simulable quantum dynamics problems. Given a spin-1/2 Hamiltonian, we show that one may define an equivalence relation on the set of Pauli strings, such that the span of each equivalence class is closed with respect to commutation with the Hamiltonian. We then study how specific Hamiltonians segregate the space of Pauli strings into these equivalence classes and compute the corresponding OEDs for operators within these classes. We provide a procedure to exactly derive these polynomials, offering a clear method to bound from above the complexity of operator evolution. Such knowledge of OEDs gives insight into the complexity of quantum dynamics of the system, which we illustrate on several models, including some which are non-free fermion models.

Equivalence classes of Pauli strings In the operator space of L spin-1/2 particles, we define a Pauli string as $P = S_1 \otimes \cdots \otimes S_L$, where $S_i \in \{I_i, X_i, Y_i, Z_i\}$. Here X_i, Y_i, Z_i are Pauli matrices acting on i th site and I_i is the identity matrix. There are 4^L different Pauli strings in total that constitute a complete operator basis $\mathcal{P} =$

$\{P_n\}_{n=1}^{4^L}$.

Consider an operator $A \in \mathcal{P}$, such that $A \equiv P_n$. The aim in a time dynamical problem is to find the Heisenberg representation of this operator $A(t)$, given by following expansion:

$$A(t) \equiv \sum_{m=1}^D f_m(t) P_m, \quad (1)$$

where $f_m(t)$ are time-dependent functions that should be obtained from the solutions of Heisenberg equations and D is the OED of the operator A . The evolution is governed by the Hamiltonian H that can be represented as a sum of M Pauli strings,

$$H = \sum_{n=1}^M h_n H_n, \quad (2)$$

where $H_n \in \mathcal{P}$ are Pauli strings (referred to as Hamiltonian strings) and h_n are real numbers.

Given the set of Hamiltonian strings $\mathcal{H} = \{H_n\}_{n=1}^M$, we can define an equivalence relation among Pauli strings (denoted by \sim) within the set \mathcal{P} . Specifically, we consider strings P_n and P_m as equivalent if they coincide or if one can be derived from another after Q rounds of commutation with Hamiltonian strings from \mathcal{H} . More specifically, there exists $\{H_{k_1}, \dots, H_{k_Q}\} \in \mathcal{H}$ and a complex number a such that:

$$P_n = a[H_{k_Q}, \dots, [H_{k_2}, [H_{k_1}, P_m]] \dots]. \quad (3)$$

This binary relation satisfies the axioms of equivalence relations. This implies reflexivity $P_n \sim P_n$, symmetry¹ $P_n \sim P_m \iff P_m \sim P_n$, and transitivity: if $P_n \sim P_m$ and $P_m \sim P_l$ then $P_n \sim P_l$.

The above equivalence relation results in a partition of \mathcal{P} into K disjoint equivalence classes $\mathcal{P} = \mathcal{A}^1 \cup \dots \cup \mathcal{A}^K$. We will employ the notation $\mathcal{A}[A]$ for equivalence classes, where A is some particular Pauli string from this class, the corresponding OED is denoted as $D[A]$. Note that to define an equivalence class, it is sufficient to specify just one operator from that class. In general, for a given Hamiltonian, the equivalence class of any operator can be determined by algorithmically generating all strings that result from commutation with the Hamiltonian strings (see Supplementary Material).

Disordered XY-spin chains. Let us consider a simple application of the equivalence class framework by examining the disordered XY-spin chain, with Hamiltonian

$$H_{XY} = \sum_{i=1}^L J_i^{xx} X_i X_{i+1} + J_i^{yy} Y_i Y_{i+1} + J_i^{xy} X_i Y_{i+1} + J_i^{yx} Y_i X_{i+1} + h_i^z Z_i, \quad (4)$$

¹ This follows from $[H_k, [H_k, P]] = 4P$ for any two non-commuting Pauli strings H_k and P .

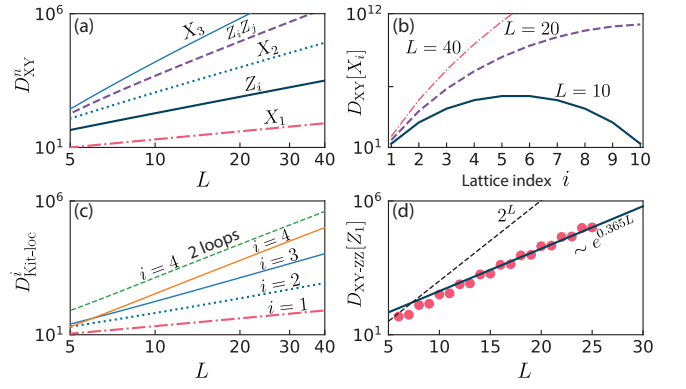


FIG. 1. The growth of OEDs for various operators as a function of the system size L and lattice index i . Log-log plot illustrating the (a) OEDs of different operators as labeled in the XY chain (4); (b) OEDs of operators X_i in the XY chain $\mathcal{A}_{XY}[X_i]$ as a function of lattice index i ; (c) sum of OEDs for single site operators in the Kitaev chain $D_{\text{Kit-loc}}^i = D_{\text{Kit}}[X_i] + D_{\text{Kit}}[Y_i] + D_{\text{Kit}}[Z_i]$. (d) Semi-log plot showing numerically obtained values of OEDs for Z_1 operator in the XY-ZZ chain and the corresponding exponential fit $\sim 11.03e^{0.365413L}$.

Here the J and h coefficients take arbitrary real values. Unless stated otherwise, we will assume open boundary conditions.

We start with the well-known classes \mathcal{A}_{XY}^1 and \mathcal{A}_{XY}^2 , which can be generated from the strings X_1 and Z_i , respectively. The class \mathcal{A}_{XY}^1 is known as Majorana strings and has the following elements:

$$\mathcal{A}_{XY}^1 = \{X_1, Z_1 X_2, Z_1 Z_2 X_3, \dots, Z_1 \dots Z_{L-1} X_L, Y_1, Z_1 Y_2, Z_1 Z_2 Y_3, \dots, Z_1 \dots Z_{L-1} Y_L\}, \quad (5)$$

which has dimension $D_{XY}^1 = 2L$. The class \mathcal{A}_{XY}^2 consists of special Pauli strings known as Onsager strings [53, 54]. An Onsager string is either a single Pauli matrix Z_j or a product of Pauli matrices on consecutive sites with matrices X or Y at the ends and matrices Z in the middle, e.g. $Y_3 Z_4 Z_5 Z_6 X_7$. There are $D_{XY}^2 = 2L^2 - L$ Onsager strings. Both these classes have an OED that are low-order polynomials in L . This can be considered the fundamental reason that particular observables in these classes can be simulated efficiently.

Interestingly, these are not the only classes that are present for the XY Hamiltonian. In fact we find that \mathcal{P} is divided into $K = 2L + 1$ equivalence classes as $\mathcal{P} = \mathcal{A}_{XY}^0 \cup \dots \cup \mathcal{A}_{XY}^{2L}$. The full set of classes can be denoted by $\mathcal{A}_{XY}^{2n-1} \equiv \mathcal{A}_{XY}[X_n]$ and $\mathcal{A}_{XY}^{2n} \equiv \mathcal{A}_{XY}[\prod_{m=1}^n Z_m]$, where $n \in [1, L]$. In addition to these there is also the trivial identity class $\mathcal{A}_{XY}^0 = \{I_1 \otimes \dots \otimes I_L\}$ which is always present in any model.

Let us now determine the dimension of these equivalence classes (see also Supplementary Material [55]). For an arbitrary system size L , the OED of the equivalence

class \mathcal{A}_{XY}^N can be written as a polynomial of degree N :

$$D_{XY}^N(L) = \sum_{j=0}^N k_j^N L^j. \quad (6)$$

The coefficients k_0^N, \dots, k_N^N for $N \leq L$ are determined as solutions of the following system of equations:

$$V(0, \dots, N) \vec{K}^N = \vec{D}_{XY}^N. \quad (7)$$

Here $V(0, 1, \dots, N)$ is a Vandermonde matrix, $\vec{K}^N \equiv (k_0^N, \dots, k_N^N)$, and the vector of values $\vec{D}_{XY}^N = (D_{XY}^N(0), \dots, D_{XY}^N(N))$ is given by

$$D_{XY}^N(m) = \begin{cases} 0 & m \leq \lceil N/2 - 1 \rceil \\ D_{XY}^{\lceil 2(m-N/2) \rceil}(m) & m \geq \lceil N/2 \rceil \\ 4^N - 2 \sum_{n=0}^{N-1} D_{XY}^n(m) & m = N \end{cases}. \quad (8)$$

For a specific N , the vector of values is determined from the previous $N - 1$ polynomials. Specifically, $D_{XY}^N(m)$ is equal to zero for the first several values of m , as on a lattice of length m there is simply no equivalence class that corresponds to N . The remaining values are determined from the relation $D_{XY}^n = D_{XY}^{2L-n}$. The same relation provides the polynomial in the case $N \geq L + 1$. The last line in (8) is derived from the fact that the sum of dimensions of all classes must be equal to 4^L . Therefore, starting from classes \mathcal{A}_{XY}^1 and \mathcal{A}_{XY}^2 one can iteratively construct all the other classes and compute their dimensionalities. Despite the extensive research history of some of these models, to our knowledge the complexity of arbitrary local operators has not been discussed.

For example, the expression for D_{XY}^5 is found to be:

$$D_{XY}^5 = \frac{4}{10}L - \frac{5}{3}L^2 + \frac{7}{3}L^3 - \frac{4}{3}L^4 + \frac{4}{15}L^5. \quad (9)$$

The above integer-valued polynomial gives the OED of the operators X_3 and Y_3 . This means that determining the exact dynamics of these operators in the basis of Pauli strings would require solving D_{XY}^5 linear equations. Figure 1(a) shows some other examples on a logarithmic plot, showing the polynomial growth of these equivalence classes. For an arbitrary lattice index X_n , the dimensionality of the corresponding class is given by a polynomial of degree $2n - 1$. In a computational complexity sense, this makes calculating the dynamics of any arbitrary Pauli string in the XY chain efficient, in the sense that the OED is polynomial. However, towards the middle of the chain the degree of the polynomial may be prohibitively large such that practically larger chains are inaccessible. In Fig. 1(b), we plot the dependence of $D_{XY}[X_i]$ on the lattice index i , showing a peak in the

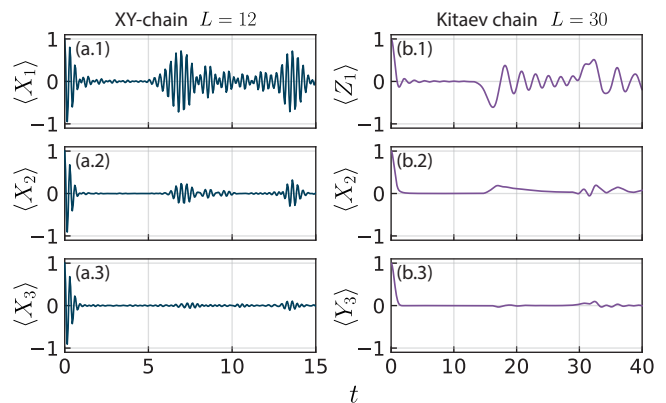


FIG. 2. Single-qubit relaxation dynamics for the initial state $\rho_{\text{init}} = |\psi_i\rangle\langle\psi_i| \otimes I^{\otimes L-1}/2^{L-1}$, here $|\psi_i\rangle$ is the state of i -th qubit, the rest of the system is at the infinite temperature. (a) XY -chain (4), $J_i^{\alpha\beta} = 1$, $h_i^z = 10$, $L = 12$, $|\psi_i\rangle = |+\rangle_i$ (b) 1D Kitaev chain (10), $J_i^x = J_i^y = J_i^z = 1$, $L = 30$, $|\psi_1\rangle = |1\rangle_1$, $|\psi_2\rangle = |+\rangle_2$, $|\psi_3\rangle = |-\rangle_3$.

middle of the chain and smaller values near the edges. This example demonstrates the edge-to-bulk growth of OED within the XY -chain. This implies the greater computational overhead to study dynamics of observables in the bulk of the system.

To show that the increase in complexity from the edge to the bulk has also physical ramifications, we compute the relaxation dynamics of a single qubit at infinite temperature. The XY chain is known to have boundary modes that are fully decoupled from the bulk excitations [49, 52]. As such we expect qubits on the edges to maintain coherence to a better extent than those in the bulk. We consider the XY Hamiltonian with the uniform couplings $J_i^{\alpha\beta} = 1$ and a large magnetic field $h_i^z = 10$, to induce fast oscillations in the XY -plane so that we may observe the coherence decay [56, 57]. As the initial state, we consider $\rho_{\text{init}} \propto |+\rangle_i\langle+| \otimes I^{\otimes L-1}$, that corresponds to i th qubit being fully polarized along x -axis and the rest of the system being at the infinite temperature state. Although the system under consideration is integrable, a single qubit placed inside an infinite temperature bath still rapidly relaxes to its equilibrium value. This, however, does not occur for the edge qubit, as its evolution takes place in a small subspace that is decoupled from the bulk. This is manifested by the collapse and revival it undergoes during evolution, as seen in Fig. 2(a.1). We observe that qubits adjacent to the edge qubit also exhibit collapse and revival, although they are less pronounced, with the amplitude vanishing as one moves towards the bulk, see Fig. 2(a.2)(a.3). The revivals can be explained by the fact that the OED of the corresponding operator near the edge is still relatively small, so the initial qubit polarization cannot dissipate swiftly due to the limited number of degrees of freedom available for dissipation.

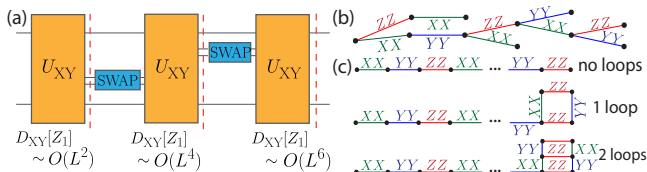


FIG. 3. (a) Growth of OED $D_{XY}[Z_1]$ of the Z_1 operator during the SWAP gate perturbed XY -evolution. Blocks $U_{XY} = e^{-itH_{XY}}$ describe evolution governed by the Hamiltonian (4). As nearest-neighbour SWAP gates are applied, $D_{XY}[Z_1]$ increases as $O(L^{2+2m})$, where m is the number of applied gates. (b) Illustration of a Kitaev Hamiltonian (10) on the tree. (c) Geometry of 1D Kitaev chains with and without loops.

Mixing of equivalence classes by perturbations and quenches. Introducing perturbations to a Hamiltonian affects the equivalence classes of the model. For example, applying periodic boundary conditions to the Hamiltonian (4) changes the equivalence classes such that instead of having a unique class for each operator X_n , only two classes distinguished by odd and even lattice indices are present, each exhibiting exponential dimensionality 4^{L-1} . The class \mathcal{A}_{XY}^2 remains composed of Onsager strings, but since the lattice is periodic its dimensionality doubles, resulting in $D_{XY-PBC}^2 = 2D_{XY}^2$. This example illustrates how the same perturbation can affect OEDs of different operators in a drastically different way.

Another example of a perturbation is applying SWAP-quenches, when a XY Hamiltonian evolution is interrupted by a nearest-neighbour SWAP-gate, see Fig. 3(a). Examining the equivalence classes of Z_i , it is found that a single SWAP $_{j,j+1}$ -gate application merges classes \mathcal{A}_{XY}^2 and \mathcal{A}_{XY}^4 , into a unified class with the dimension being fourth order in L . Generally, applying multiple SWAP-quenches during XY evolution increases the OED of Z_i as polynomial of degree $2 + 2m$, with m representing the number of quenches. This is consistent with the asymptotic results recently reported in [58]. Ultimately, SWAP-quenches will intermix all equivalence classes into one, achieving a dimensionality of $4^L - 1$. This is consistent with the fact that XY dynamics combined with SWAP-quenches is universal [46].

Not all quenches, however, merge equivalence classes. One example of this are parameter quenches in (2) $h_n \rightarrow h'_n$ do not affect worst case OED. Due to this fact our formalism is directly extendable to time-dependent Hamiltonians. Another example are Pauli gates $W = X_i, Y_i, Z_i$ which act on any Pauli string as $W^\dagger P_n W = \pm P_n$, leaving any equivalence class of Pauli strings unaffected. In case of the class \mathcal{A}_{XY}^2 , it is easy to check that the phase gate $W = \sqrt{Z_i}$ and the gate $W = X_i \cos \alpha + Y_i \sin \alpha$, where $\alpha \in \mathbb{R}$, are also equivalence preserving quenches. Therefore XY dynamics can be augmented with an arbitrary number of the above quenches without complicating its

simulability.

Other Hamiltonians. To show that our methods are applicable in a more general context, we consider other Hamiltonians. One example is the Kitaev Hamiltonian on a tree graph G_{tree}^L with L vertexes and at most three edges incident to each vertex (Fig. 3(b)). The Hamiltonian has the form [59]

$$H_{\text{Kit}} = \sum_{\langle i,j \rangle \in G} J_{ij}^x X_i X_j + J_{ij}^y Y_i Y_j + J_{ij}^z Z_i Z_j, \quad (10)$$

where for a given pair $\langle i,j \rangle$ of neighbouring vertexes two of three coupling constants $J_{ij}^{x,y,z}$ must be zero, but the remaining is non-zero. In addition, the Hamiltonian must have a proper 3-edge coloring of the graph, where each ‘‘color’’ represents the interaction type XX, YY or ZZ , and proper coloring implies that no vertex belongs to two edges with the same color. For this Hamiltonian, each local operator X_n, Y_n or Z_n belongs to its unique equivalence class and has OEDs that can be given as at most n th degree polynomial of L . In Fig. 1(c) the growth of the OED for local Pauli operators is shown for the one-dimensional Kitaev chain (Fig. 3(c)), revealing a polynomial growth of $D_{\text{Kit-loc}}^n$. We find that OEDs of local operators in the Hamiltonian (10) can always be expressed as an integer-valued polynomial as long as the tree structure of the Hamiltonian is maintained, with the specific geometry influencing the form of the polynomial.

Kitaev Hamiltonians such as (10) offer a rich playground for exploring equivalence classes and the dynamics of operator growth. Such Hamiltonians contain numerous local operators that belong to equivalence classes of relatively low dimensions. Introducing external magnetic fields or loops in the graph one can merge some of these classes in a controllable manner. For example, in Fig. 1(c) we demonstrate how the total OEDs of local operators X_4, Y_4, Z_4 increases when the tree structure of the graph in the Hamiltonian (10) is disrupted by adding loops while maintaining its length (Fig. 3(c)). This results in a dimensional jump of $D_{\text{Kit-loc}}^n$ by a factor of $2^m D_{\text{Kit-loc}}^n$, where m denotes the number of added loops. This relation holds within range of n and m , as long as $2^m D_{\text{Kit-loc}}^n \ll 4^L$.

Finally, we introduce the $XY - ZZ$ model which again induces a nontrivial division of equivalence classes. The Hamiltonian of $XY - ZZ$ model reads:

$$H_{XY-ZZ} = \sum_{i=1}^L J_{2i-1}^x X_{2i-1} X_{2i} + J_{2i-1}^y Y_{2i-1} Y_{2i} + J_{2i}^z Z_{2i} Z_{2i+1}, \quad (11)$$

here again the coefficients J are real. In case of this Hamiltonian the operators X_i and Y_i each belong to distinct equivalence classes with dimensionalities $D_{XY-ZZ}[X_i, Y_i] = 4^{L-3}$. Pairs of operators Z_{2i-1} and Z_{2i} for $i > 1$, belong to equivalence classes with slightly bigger dimensionality scaling as $O(4^{L-3})$. While the OED

of these classes are exponentially growing, some grow at a much slower rate 2^L . The most intriguing case involves the edge operator Z_1 , whose equivalence class dimensionality grows approximately as $D_{XY-ZZ}[Z_1] \simeq 11e^{0.365L}$, see Fig 1(d). The factor 0.365 in the exponent enables a significant practical reduction in problem complexity, compared to exact diagonalization. For example, if one were to calculate the dynamics of $Z_1(t)$ using exact diagonalization, even for a fixed initial state, it would require $O(2^L)$ resources. Suppose that one has enough computational power to perform exact diagonalization for 30 qubits, then by solving Heisenberg equations inside of the equivalence class $\mathcal{A}_{XY-ZZ}^{Z_1}$ one could find $Z_1(t)$ for up to 45 qubits with the same resources.

Discussion. We have developed a formalism of equivalence classes which allows one to obtain the dimension of the operator evolution in the Heisenberg picture for spin-1/2 Hamiltonians. The approach gives a straightforward way of understanding the nature of why particular models can be time integrable, and provides a powerful tool for identifying when quantum dynamics are simulable. To illustrate our approach we examined well-studied models such as the XY and Kitaev chains and recovered the known result that X_i, Y_i at the chain ends and all Z_i can be efficiently computed. Despite the long history of these models, to our knowledge, the remaining equivalence classes have not been identified to date. We showed that the X_i, Y_i observables increase in complexity moving from edge to bulk. We also considered various perturbations that may or may not affect the OEDs of certain operators. We showed that applications of certain single-qubit gates during the evolution do not affect OED of some operators under simulation. This is interesting from a quantum circuit point of view as it implies that matchgate circuits can be augmented with such gates without penalty regarding the simulation. We examined universality-enabling gates for XY evolution, specifically SWAP gates, which increases the degree of the OED linearly with the number of SWAP gates. Similarly, loops on Kitaev model on trees increases the complexity by an exponential factor in the number of loops.

To illustrate our results we mainly showed results on free-fermionic models, but they may also be applied in other contexts. We introduced the non-free fermion $XY-ZZ$ model, we showed that all equivalence classes have exponential dimensionality. In this model, almost each local operator still resides within its own equivalence class. Moreover, the z -projections of edge qubits also have OEDs that scale more slowly than those of bulk qubits. Solving the dynamics within the corresponding equivalence class will still significantly outperform brute force approach that disregard the spitting of the operator space, such as exact diagonalization. While we focused on the basis of Pauli strings for simplicity in this paper, it is important to note that operators with small OED exist in other bases as well [34, 39, 60, 61]. Therefore,

studying the separation of other bases into equivalence classes may potentially yield more examples of simulable quantum dynamics.

I. E. and O. L. are supported by Rosatom in the framework of the Roadmap for Quantum computing (Contract No. 868-1.3-15/15-2021 dated October 5, 2021). Part of the work presented in paragraph “Disordered XY -spin chains” was supported by the Foundation for the Advancement of Theoretical Physics and Mathematics “BASIS” under the grant N 22-1-2-55-1. T. B. is supported by the National Natural Science Foundation of China (62071301); NYU-ECNU Institute of Physics at NYU Shanghai; Shanghai Frontiers Science Center of Artificial Intelligence and Deep Learning; the Joint Physics Research Institute Challenge Grant; the Science and Technology Commission of Shanghai Municipality (19XD1423000, 22ZR1444600); the NYU Shanghai Boost Fund; the China Foreign Experts Program (G2021013002L); the NYU Shanghai Major-Grants Seed Fund; Tamkeen under the NYU Abu Dhabi Research Institute grant CG008; and the SMEC Scientific Research Innovation Project (2023ZKZD55).

* tim.byrnes@nyu.edu

† lychkovskiy@gmail.com

- [1] B. Swingle, Unscrambling the physics of out-of-time-order correlators, *Nature Physics* **14**, 988 (2018).
- [2] D. E. Parker, X. Cao, A. Avdoshkin, T. Scaffidi, and E. Altman, A universal operator growth hypothesis, *Physical Review X* **9**, 041017 (2019).
- [3] J. Li, R. Fan, H. Wang, B. Ye, B. Zeng, H. Zhai, X. Peng, and J. Du, Measuring out-of-time-order correlators on a nuclear magnetic resonance quantum simulator, *Physical Review X* **7**, 031011 (2017).
- [4] C. W. von Keyserlingk, T. Rakovszky, F. Pollmann, and S. L. Sondhi, Operator hydrodynamics, otocs, and entanglement growth in systems without conservation laws, *Physical Review X* **8**, 021013 (2018).
- [5] A. Nahum, S. Vijay, and J. Haah, Operator spreading in random unitary circuits, *Physical Review X* **8**, 021014 (2018).
- [6] V. Khemani, A. Vishwanath, and D. A. Huse, Operator spreading and the emergence of dissipative hydrodynamics under unitary evolution with conservation laws, *Physical Review X* **8**, 031057 (2018).
- [7] I. MacCormack, M. T. Tan, J. Kudler-Flam, and S. Ryu, Operator and entanglement growth in nonthermalizing systems: Many-body localization and the random singlet phase, *Physical Review B* **104**, 214202 (2021).
- [8] F. Ballar Trigueros and C.-J. Lin, Krylov complexity of many-body localization: Operator localization in krylov basis, *SciPost Physics* **13**, 037 (2022).
- [9] I. García-Mata, R. A. Jalabert, and D. A. Wisniacki, Out-of-time-order correlators and quantum chaos, arXiv preprint arXiv:2209.07965 (2022).
- [10] T. Zhou and B. Swingle, Operator growth from global out-of-time-order correlators, *Nature communications*

- 14, 3411 (2023).
- [11] F. Uskov and O. Lychkovskiy, Quantum dynamics in one and two dimensions via recursion method, arXiv preprint arXiv:2401.17211 (2024).
- [12] Y.-L. Zhang, Y. Huang, X. Chen, *et al.*, Information scrambling in chaotic systems with dissipation, *Physical Review B* **99**, 014303 (2019).
- [13] B. Yoshida and N. Y. Yao, Disentangling scrambling and decoherence via quantum teleportation, *Physical Review X* **9**, 011006 (2019).
- [14] A. Touil and S. Deffner, Information scrambling versus decoherence—two competing sinks for entropy, *PRX Quantum* **2**, 010306 (2021).
- [15] T. Schuster and N. Y. Yao, Operator growth in open quantum systems, *Phys. Rev. Lett.* **131**, 160402 (2023).
- [16] T. Rakovszky, C. W. von Keyserlingk, and F. Pollmann, Dissipation-assisted operator evolution method for capturing hydrodynamic transport, *Phys. Rev. B* **105**, 075131 (2022).
- [17] A. De, U. Borla, X. Cao, and S. Gazit, Stochastic sampling of operator growth, arXiv preprint arXiv:2401.06215 (2024).
- [18] I. Ermakov, O. Lychkovskiy, and T. Byrnes, Unified framework for efficiently computable quantum circuits, arXiv preprint arXiv:2401.08187 (2024).
- [19] F. Arute, K. Arya, R. Babbush, D. Bacon, J. C. Bardin, R. Barends, R. Biswas, S. Boixo, F. G. Brandao, D. A. Buell, *et al.*, Quantum supremacy using a programmable superconducting processor, *Nature* **574**, 505 (2019).
- [20] S. Aaronson and D. Gottesman, Improved simulation of stabilizer circuits, *Physical Review A* **70**, 052328 (2004).
- [21] S. Boixo, S. V. Isakov, V. N. Smelyanskiy, R. Babbush, N. Ding, Z. Jiang, M. J. Bremner, J. M. Martinis, and H. Neven, Characterizing quantum supremacy in near-term devices, *Nature Physics* **14**, 595 (2018).
- [22] A. Smith, M. Kim, F. Pollmann, and J. Knolle, Simulating quantum many-body dynamics on a current digital quantum computer, *npj Quantum Information* **5**, 106 (2019).
- [23] Y. Wu, W.-S. Bao, S. Cao, F. Chen, M.-C. Chen, X. Chen, T.-H. Chung, H. Deng, Y. Du, D. Fan, *et al.*, Strong quantum computational advantage using a superconducting quantum processor, *Physical review letters* **127**, 180501 (2021).
- [24] L. S. Madsen, F. Laudenbach, M. F. Askarani, F. Rortais, T. Vincent, J. F. Bulmer, F. M. Miatto, L. Neuhaus, L. G. Helt, M. J. Collins, *et al.*, Quantum computational advantage with a programmable photonic processor, *Nature* **606**, 75 (2022).
- [25] K. Xu, J.-J. Chen, Y. Zeng, Y.-R. Zhang, C. Song, W. Liu, Q. Guo, P. Zhang, D. Xu, H. Deng, *et al.*, Emulating many-body localization with a superconducting quantum processor, *Physical review letters* **120**, 050507 (2018).
- [26] L. G. Valiant, Quantum computers that can be simulated classically in polynomial time, in *Proceedings of the thirty-third annual ACM symposium on Theory of computing* (2001) pp. 114–123.
- [27] L. G. Valiant, Expressiveness of matchgates, *Theoretical Computer Science* **289**, 457 (2002).
- [28] T. Prosen, A new class of completely integrable quantum spin chains, *Journal of Physics A: Mathematical and General* **31**, L397 (1998).
- [29] B. Zunkovic, Closed hierarchy of correlations in Markovian open quantum systems, *New Journal of Physics* **16**, 013042 (2014).
- [30] M. Foss-Feig, J. T. Young, V. V. Albert, A. V. Gorshkov, and M. F. Maghrebi, Solvable family of driven-dissipative many-body systems, *Phys. Rev. Lett.* **119**, 190402 (2017).
- [31] N. Shibata and H. Katsura, Dissipative spin chain as a non-Hermitian Kitaev ladder, *Phys. Rev. B* **99**, 174303 (2019).
- [32] P. E. Dolgirev, J. Marino, D. Sels, and E. Demler, Non-gaussian correlations imprinted by local dephasing in fermionic wires, *Phys. Rev. B* **102**, 100301 (2020).
- [33] F. H. L. Essler and L. Piroli, Integrability of one-dimensional lindbladians from operator-space fragmentation, *Phys. Rev. E* **102**, 062210 (2020).
- [34] O. Lychkovskiy, Closed hierarchy of heisenberg equations in integrable models with onsager algebra, *SciPost Physics* **10**, 124 (2021).
- [35] A. A. Budini and J. P. Garrahan, Solvable class of non-markovian quantum multipartite dynamics, *Phys. Rev. A* **104**, 032206 (2021).
- [36] O. Gamayun, A. Slobodeniuk, J.-S. Caux, and O. Lychkovskiy, Nonequilibrium phase transition in transport through a driven quantum point contact, *Physical Review B* **103**, L041405 (2021).
- [37] C. Guo and D. Poletti, Analytical solutions for a boundary-driven x y chain, *Physical Review A* **98**, 052126 (2018).
- [38] B. Horstmann, J. I. Cirac, and G. Giedke, Noise-driven dynamics and phase transitions in fermionic systems, *Physical Review A* **87**, 012108 (2013).
- [39] O. Gamayun and O. Lychkovskiy, Out-of-equilibrium dynamics of the kitaev model on the bethe lattice via coupled heisenberg equations, *SciPost Physics* **12**, 175 (2022).
- [40] A. Teretenkov and O. Lychkovskiy, Exact dynamics of quantum dissipative xx models: Wannier-stark localization in the fragmented operator space, *Phys. Rev. B* **109**, L140302 (2024).
- [41] M. Žnidarič, Exact solution for a diffusive nonequilibrium steady state of an open quantum chain, *Journal of Statistical Mechanics: Theory and Experiment* **2010**, L05002 (2010).
- [42] M. Žnidarič and M. Horvat, Transport in a disordered tight-binding chain with dephasing, *The European Physical Journal B* **86**, 1 (2013).
- [43] I. Ermakov and O. Lychkovskiy, Effect of dephasing on the current through a periodically driven quantum point contact, *JETP Letters* **119**, 40 (2024).
- [44] R. Ghosh and M. Žnidarič, Relaxation of imbalance in a disordered xx model with on-site dephasing, *Physical Review B* **107**, 184303 (2023).
- [45] J. a. Ferreira, T. Jin, J. Mannhart, T. Giamarchi, and M. Filippone, Transport and nonreciprocity in monitored quantum devices: An exact study, *Phys. Rev. Lett.* **132**, 136301 (2024).
- [46] R. Jozsa and A. Miyake, Matchgates and classical simulation of quantum circuits, *Proceedings of the Royal Society A: Mathematical, Physical and Engineering Sciences* **464**, 3089 (2008).
- [47] R. Jozsa and M. V. d. Nest, Classical simulation complexity of extended clifford circuits, arXiv preprint arXiv:1305.6190 (2013).
- [48] D. J. Brod, Efficient classical simulation of matchgate cir-

- cuits with generalized inputs and measurements, *Physical Review A* **93**, 062332 (2016).
- [49] A. Y. Kitaev, Unpaired majorana fermions in quantum wires, *Physics-uspekhi* **44**, 131 (2001).
- [50] P. Fendley, Strong zero modes and eigenstate phase transitions in the xyz/interacting majorana chain, *Journal of Physics A: Mathematical and Theoretical* **49**, 30LT01 (2016).
- [51] P. Fendley, Parafermionic edge zero modes in zn-invariant spin chains, *Journal of Statistical Mechanics: Theory and Experiment* **2012**, P11020 (2012).
- [52] X. Mi, M. Sonner, M. Y. Niu, K. W. Lee, B. Foxen, R. Acharya, I. Aleiner, T. I. Andersen, F. Arute, K. Arya, *et al.*, Noise-resilient edge modes on a chain of superconducting qubits, *Science* **378**, 785 (2022).
- [53] D. K. Jha and J. G. Valatin, XY model and algebraic methods, *Journal of Physics A: Mathematical, Nuclear and General* **6**, 1679 (1973).
- [54] A. Teretenkov and O. Lychkovskiy, Exact dynamics of quantum dissipative xx models: Wannier-stark localization in the fragmented operator space, *Physical Review B* **109**, L140302 (2024).
- [55] See the Supplementary Material.
- [56] Z.-H. Ma, J. Cui, Z. Cao, S.-M. Fei, V. Vedral, T. Byrnes, and C. Radhakrishnan, Operational advantage of basis-independent quantum coherence, *Europhysics Letters* **125**, 50005 (2019).
- [57] C. Radhakrishnan, Z. Ding, F. Shi, J. Du, and T. Byrnes, Basis-independent quantum coherence and its distribution, *Annals of Physics* **409**, 167906 (2019).
- [58] A. Mocherla, L. Lao, and D. E. Browne, Extending matchgate simulation methods to universal quantum circuits, arXiv preprint arXiv:2302.02654 (2023).
- [59] A. Kitaev, Anyons in an exactly solved model and beyond, *Annals of Physics* **321**, 2 (2006), january Special Issue.
- [60] D. B. Uglov and I. T. Ivanov, sl (n) onsager's algebra and integrability, *Journal of statistical physics* **82**, 87 (1996).
- [61] Y. Miao, Generalised onsager algebra in quantum lattice models, *SciPost Physics* **13**, 070 (2022).

Supplementary material for: Polynomially restricted operator growth in dynamically integrable models

Igor Ermakov,^{1,2} Tim Byrnes,^{3,4,5,6,*} and Oleg Lychkovskiy^{7,1,2,†}

¹*Russian Quantum Center, Skolkovo, Moscow 121205, Russia*

²*Department of Mathematical Methods for Quantum Technologies, Steklov Mathematical Institute of Russian Academy of Sciences, 8 Gubkina St., Moscow 119991, Russia.*

³*New York University Shanghai, NYU-ECNU Institute of Physics at NYU Shanghai, Shanghai Frontiers Science Center of Artificial Intelligence and Deep Learning, 567 West Yangsi Road, Shanghai, 200126, China.*

⁴*State Key Laboratory of Precision Spectroscopy, School of Physical and Material Sciences, East China Normal University, Shanghai 200062, China*

⁵*Center for Quantum and Topological Systems (CQTS),*

NYUAD Research Institute, New York University Abu Dhabi, UAE.

⁶*Department of Physics, New York University, New York, NY 10003, USA*

⁷*Skolkovo Institute of Science and Technology, Bolshoy Boulevard 30, bld. 1, Moscow 121205, Russia.*

(Dated: June 18, 2024)

ALGORITHMIC GENERATION OF EQUIVALENCE CLASSES

Let us introduce the basis of Pauli string P as $P = S_1 \otimes \cdots \otimes S_L$, where $S_i \in \{I_i, X_i, Y_i, Z_i\}$, here X_i, Y_i, Z_i are Pauli matrices acting on i th site, I_i is the identity matrix. There are 4^L different Pauli strings in total that constitute a complete basis $\mathcal{P} = \{P_n\}_{n=1}^{4^L}$. Let us also introduce an inner product $\langle\langle \cdot, \cdot \rangle\rangle$ in this basis as:

$$\langle\langle P_i, P_j \rangle\rangle \equiv \text{tr}(P_i^\dagger P_j) / \text{tr}(\mathbb{I}) = \delta_{ij}. \quad (\text{S1})$$

We assume that the Hamiltonian H can be represented as a sum of N Pauli strings,

$$H = \sum_{n=1}^N h_n H_n, \quad (\text{S2})$$

where $H_n \in \mathcal{P}$ are Pauli string (referred to as *Hamiltonian strings* in what follows) and h_n are real numbers.

Now, we will construct a closed subset \mathcal{A} starting from some seed operator $A_1 \in \mathcal{P}$. To this end, we implement Algorithm 1. Algorithm 1 adds new Pauli strings obtained from the commutation with strings from \mathcal{H} to the set \mathcal{A} if they are not already in the set. The algorithm stops when no new string can be generated. As a result of this algorithm, we obtain subset \mathcal{A} of dimensionality D , which is closed with respect to the commutation with H .

For a finite L , this algorithm must always stop because in this case, the algorithm can generate only $4^L - 1$ strings at most. Note that the identity Pauli string $I^{(1)} = \mathbb{I} \equiv I_1 \otimes \cdots \otimes I_L$ is a trivial integral of motion and can never be generated as a commutation of two other strings. In the simplest case, when A_1 is the integral of motion and therefore commutes with the Hamiltonian, no new strings will be added to \mathcal{A} , thus $D = 1$.

After constructing the equivalence class $\mathcal{A} = \{A_1, \dots, A_D\}$, we can write down the Heisenberg equations in a vectorized form as follows:

$$\frac{d}{dt} A(t) = M A(t), \quad (\text{S3})$$

where we introduced vector A composed of operators as $A = (A_1, \dots, A_D)$, and $A(0), A(t)$ are Schrödinger and Heisenberg representations correspondingly. The elements of matrix M are defined as follows:

$$m_{ij} = \sum_{n=1}^N i h_n \langle\langle A_j, [H_n, A_i] \rangle\rangle. \quad (\text{S4})$$

It can be easily verified that matrix M is real and skew-symmetric, $m_{ij} = m_{ij}^* = -m_{ji}$.

To find $A_i(t)$, one must further compute the matrix exponential $S(t) = e^{Mt}$. After this, the solution of (S3) can be found as

$$A_i(t) = \sum_{j=1}^D s_{ij}(t) A_j(0), \quad (\text{S5})$$

Algorithm 1 Generation of basis

Require: Fix A_1 and $\mathcal{H} = \{H_n\}_{n=1}^N$

$D = 1$

counter = 0

while counter < D **do**

$V = \mathcal{A}[\text{counter} + 1]$

for $n = 1, n \leq N, n = n + 1$ **do**

$[H_n, V] = aA$

if $a \neq 0$ and $A \notin \mathcal{A}$ **then**

$\mathcal{A} \leftarrow A$

▷ Add A to the subset

$D = D + 1$

end if

end for

counter = counter + 1

end while

where $s_{ij}(t)$ are matrix elements of $S(t)$. Notice that computing the matrix exponential of $M(t)$ requires additional computational effort, although polynomial in D . However, if one is only interested in the expectation values $\langle A_i \rangle(t) \equiv \text{tr}(A_i(t)\rho_{\text{ini}})$ for a specific initial state ρ_{ini} , then direct integration of (S3) can be performed, which is a computationally easier task.

DIMENSIONALITIES OF EQUIVALENCE CLASSES IN THE XY CHAIN

The Hamiltonian of XY chain is given by:

$$H_{XY} = \sum_{i=1}^L J_i^{xx} X_i X_{i+1} + J_i^{yy} Y_i Y_{i+1} + J_i^{xy} X_i Y_{i+1} + J_i^{yx} Y_i X_{i+1} + h_i^z Z_i, \quad (\text{S6})$$

We will assume open boundary conditions if not stated otherwise.

Majorana and Onsager strings

There is always a trivial class \mathcal{A}_{XY}^0 which consists of identity operator $I^{(1)} = I_1 \dots I_L$, the dimensionality of this class is $D_{XY}^0 = 1$.

Let us start with the class of Majorana strings \mathcal{A}_{XY}^1 which can be generated from the operator X_1 . The class \mathcal{A}_{XY}^1 has the following structure:

$$\mathcal{A}_{XY}^1 = \{X_1, Z_1 X_2, Z_1 Z_2 X_3, \dots, Z_1 \dots Z_{L-1} X_L, \\ Y_1, Z_1 Y_2, Z_1 Z_2 Y_3, \dots, Z_1 \dots Z_{L-1} Y_L\}, \quad (\text{S7})$$

with the dimensionality of $D_{XY}^1 = 2L$.

The class of Onsager strings \mathcal{A}_{XY}^2 has the following structure:

$$\mathcal{A}_{XY}^2 = \left\{ \left\{ R_j^n \right\}_{j=1, n=1-L}^{L-n, L-1}, \left\{ Q_j^n \right\}_{j=1, n=1-L, n \neq 0}^{L-n, L-1} \right\}, \quad (\text{S8})$$

where R_j^n and Q_j^n are defined as

$$\begin{aligned}
R_j^0 &= Z_j \\
R_j^{-n} &= Y_j \left(\prod_{m=1}^{n-1} Z_{j+m} \right) Y_{j+n}, \\
R_j^n &= X_j \left(\prod_{m=1}^{n-1} Z_{j+m} \right) X_{j+n}, \\
Q_j^n &= X_j \left(\prod_{m=1}^{n-1} Z_{j+m} \right) Y_{j+n}, \\
Q_j^{-n} &= Y_j \left(\prod_{m=1}^{n-1} Z_{j+m} \right) X_{j+n}.
\end{aligned} \tag{S9}$$

The dimensionality of this class is given by the polynomial $D_{XY}^2 = 2L^2 - L$.

Mirrored classes

Equivalence classes possess particular symmetries that may be exploited to deduce their structure. We first consider the following lemma.

Lemma 1 *If a product of two Pauli strings $P_{AB} = P_A P_B$ from equivalence classes $P_A \in \mathcal{A}$ and $P_B \in \mathcal{B}$, does not belong to either of them, $P_{AB} \notin \mathcal{A} \cup \mathcal{B}$, then it belongs to an equivalence class \mathcal{AB} which consist only of products of strings from \mathcal{A} and \mathcal{B} .*

To prove the above lemma one needs to use the fact that the following is satisfied for three arbitrary Pauli strings $[P_1 P_2, P_3] = \alpha [P_1, P_3] P_2$, here $\alpha \in \mathbb{C}$. In this case let us consider some string generated from P_{AB} and some Hamiltonian string H_n :

$$[P_{AB}, H_n] \equiv [P_A P_B, H_n] = \alpha P_A [P_B, H_n], \tag{S10}$$

which is a product of two Pauli strings from \mathcal{A} and \mathcal{B} or zero.

Now, let us introduce mirrored classes in the XY chain. The Hamiltonian (S6), in general, has only one integral of motion that can be expressed as a single Pauli string, namely the operator $I^{(2)} = Z_1 \dots Z_L$ which constitutes the class \mathcal{A}_{XY}^{2L} . If one multiplies each Pauli string from an equivalence class \mathcal{A} by the integral of motion $I^{(2)}$, one obtains another, ‘‘mirrored’’ equivalence class $\bar{\mathcal{A}}$, thanks to the identity $[H_n, I^{(2)} A_k] = I^{(2)} [H_n, A_k]$. More importantly the dimensionality of the original and mirrored classes coincide. Therefore in case of XY chain we have:

$$D_{XY}^n = D_{XY}^{2L-n}, \quad n \in [0, L] \tag{S11}$$

Also it is important to note that the class \mathcal{A}_{XY}^L always coincides with its mirroring. Indeed it can be is either generated from the operator $X_{(L+1)/2}$ in case of odd L and from $Z_1 \dots Z_{L/2}$ in case of even L . Below we will also show that this class has maximal dimensionality.

Integer-valued polynomials for dimensionalities of equivalence classes

We now derive integer-valued polynomials that describe dimensionalities of equivalence classes \mathcal{A}_{XY}^n in the XY chain.

First let us consider the simplest case of single qubit $L = 1$. In this case the partition into equivalence classes given by the Hamiltonian (S6) is very simple, namely: $\mathcal{A}_{XY}^0 = \{I_1\}$, $\mathcal{A}_{XY}^1 = \{X_1, Y_1\}$ and $\mathcal{A}_{XY}^2 = \{Z_1\}$. Only L first classes are important to us, because other L classes can be obtained from them by mirroring. In case of $L = 1$ it is easy to see that \mathcal{A}_{XY}^2 is the mirror class to \mathcal{A}_{XY}^0 . Therefore it is evident that:

$$4^1 = 2D_{XY}^0(1) + D_{XY}^1(1), \quad L = 1. \tag{S12}$$

Next we consider the case of two qubits $L = 2$. In this case we have classes \mathcal{A}_{XY}^0 and \mathcal{A}_{XY}^1 as well as their mirrored classes, additionally to it we have \mathcal{A}_{XY}^2 with dimensionality D_{XY}^2 . One can check that:

$$4^2 = 2D_{XY}^0(2) + 2D_{XY}^1(2) + D_{XY}^2(2), \quad L = 2 \quad (\text{S13})$$

Let us move one to the case of $L = 3$. In this case the class \mathcal{A}_{XY}^3 generated from the operator X_2 appears. Continuing previous line of thinking one can write down:

$$4^3 = 2D_{XY}^0(3) + 2D_{XY}^1(3) + 2D_{XY}^2(3) + D_{XY}^3(3), \quad L = 3 \quad (\text{S14})$$

Unlike previous cases $L = 1, 2$, here we do not know the general expression for $D_{XY}^3(L)$. This can be obtained in the following way. The number of strings in \mathcal{A}_{XY}^3 scales as $O(L^3)$ because it must be proportional to the product of D_{XY}^1 and D_{XY}^2 . Indeed, $X_2 = Z_1 \otimes Z_1 X_2$, therefore due to the above lemma the class \mathcal{A}_{XY}^3 consists of products of strings from \mathcal{A}_{XY}^1 and \mathcal{A}_{XY}^2 . So at most \mathcal{A}_{XY}^3 can have $D_{XY}^1 D_{XY}^2$ Pauli strings. Since many products from \mathcal{A}_{XY}^1 and \mathcal{A}_{XY}^2 yield either the same Pauli string or a string from one of these classes $D_{XY}^3 < D_{XY}^1 D_{XY}^2$. Therefore, at most $D_{XY}^3(L)$ can be an integer-valued polynomial of 3rd order. Let us seek for it in the form:

$$D_{XY}^3(L) = k_0^3 + k_1^3 L + k_2^3 L^2 + k_3^3 L^3. \quad (\text{S15})$$

To determine the coefficients $k_0^3, k_1^3, k_2^3, k_3^3$, we need 4 equations. First, $D_{XY}^3(0) = 0$ and therefore $k_0^3 = 0$. This is degenerate case which yet must be considered. Second, $D_{XY}^3(1) = 0$, because no operators X_2 appear in the lattice of $L = 1$ qubit. Third equation is $D_{XY}^3(2) = D_{XY}^1(2)$, because when $L = 2$ the class \mathcal{A}_{XY}^3 generated from X_2 is the mirrored to the class \mathcal{A}_{XY}^1 . The last equation can be obtained from the expression (S14).

We therefore have the following system of equations

$$\begin{aligned} D_{XY}^3(0) &= 0 \\ D_{XY}^3(1) &= 0 \\ D_{XY}^3(2) &= D_{XY}^1(2) \\ D_{XY}^3(3) &= 4^3 - 2D_{XY}^0(3) - 2D_{XY}^1(3) - 2D_{XY}^2(3). \end{aligned} \quad (\text{S16})$$

This is the system of linear equations with respect to variables $k_0^3, k_1^3, k_2^3, k_3^3$. By solving it we obtain:

$$D_{XY}^3 = \frac{2}{3}L - 2L^2 + \frac{4}{3}L^3. \quad (\text{S17})$$

The above procedure can be generalized for the case of arbitrary D_{XY}^N . Let us look for the D_{XY}^N in the form of the following polynomial:

$$D_{XY}^N = \sum_{n=0}^N k_n^N L^n, \quad (\text{S18})$$

the coefficients k_0^N, \dots, k_N^N are found as the solution of the following system of equations, if N is odd:

$$\begin{aligned} D_{XY}^N(0) &= 0 \\ &\vdots \\ D_{XY}^N\left(\frac{N-1}{2}\right) &= 0 \\ D_{XY}^N\left(\frac{N+1}{2}\right) &= D_{XY}^1\left(\frac{N+1}{2}\right) \\ D_{XY}^N\left(\frac{N+1}{2} + 1\right) &= D_{XY}^3\left(\frac{N+1}{2} + 1\right) \\ &\vdots \\ D_{XY}^N(N-1) &= D_{XY}^{N-2}(N-1) \\ D_{XY}^N(N) &= 4^N - 2 \sum_{n=0}^{N-1} D_{XY}^n(N), \end{aligned} \quad (\text{S19})$$

and if N is even then the system changes to:

$$\begin{aligned}
D_{XY}^N(0) &= 0 \\
&\vdots \\
D_{XY}^N\left(\frac{N}{2} - 1\right) &= 0 \\
D_{XY}^N\left(\frac{N}{2}\right) &= D_{XY}^0\left(\frac{N}{2}\right) \\
D_{XY}^N\left(\frac{N}{2} + 1\right) &= D_{XY}^2\left(\frac{N}{2} + 1\right) \\
&\vdots \\
D_{XY}^N(N-1) &= D_{XY}^{N-2}(N-1) \\
D_{XY}^N(N) &= 4^N - 2 \sum_{n=0}^{N-1} D_{XY}^n(N).
\end{aligned} \tag{S20}$$

The left-hand side of the above systems can be expressed in terms of Vandermonde matrix as $V(0, \dots, N)\vec{K}^N$. The Vandermonde matrix $V(0, \dots, N)$ always have a positive determinant, ensuring that a unique solution exists.

By consequently solving this system for different N starting from 3 we can obtain expressions for first several polynomials:

$$\begin{aligned}
D_{XY}^1 &= 2L \\
D_{XY}^2 &= -L + 2L^2 \\
D_{XY}^3 &= \frac{2}{3}L - 2L^2 + \frac{4}{3}L^3 \\
D_{XY}^4 &= -\frac{1}{2}L + \frac{11}{6}L^2 - 2L^3 + \frac{2}{3}L^4 \\
D_{XY}^5 &= \frac{4}{10}L - \frac{5}{3}L^2 + \frac{7}{3}L^3 - \frac{4}{3}L^4 + \frac{4}{15}L^5 \\
D_{XY}^6 &= -\frac{1}{3}L + \frac{137}{90}L^2 - \frac{5}{2}L^3 + \frac{17}{9}L^4 - \frac{2}{3}L^5 + \frac{4}{45}L^6 \\
D_{XY}^7 &= \frac{2}{3}L - \frac{7}{5}L^2 + \frac{116}{45}L^3 - \frac{7}{3}L^4 + \frac{10}{9}L^5 - \frac{4}{15}L^6 + \frac{8}{315}L^7.
\end{aligned} \tag{S21}$$

By continuing this process one can obtain exact expressions for OEDs of any operator in the XY chain.

Scaling of the leading coefficient in D_{XY}^L

The reader might be concerned by the following: for L qubits, there is an equivalence class of maximal dimensionality D_{XY}^L scaling as $O(L^L)$. Such superexponential scaling is capable of surpassing the total number of Pauli strings, 4^L which would be a contradiction. This, however, never happens as the coefficient k_L^L in front of the leading power in the expression for D_{XY}^L also decreases superexponentially; see Fig. S1.

* Electronic address: tim.byrnese@nyu.edu

† Electronic address: lychkovskiy@gmail.com

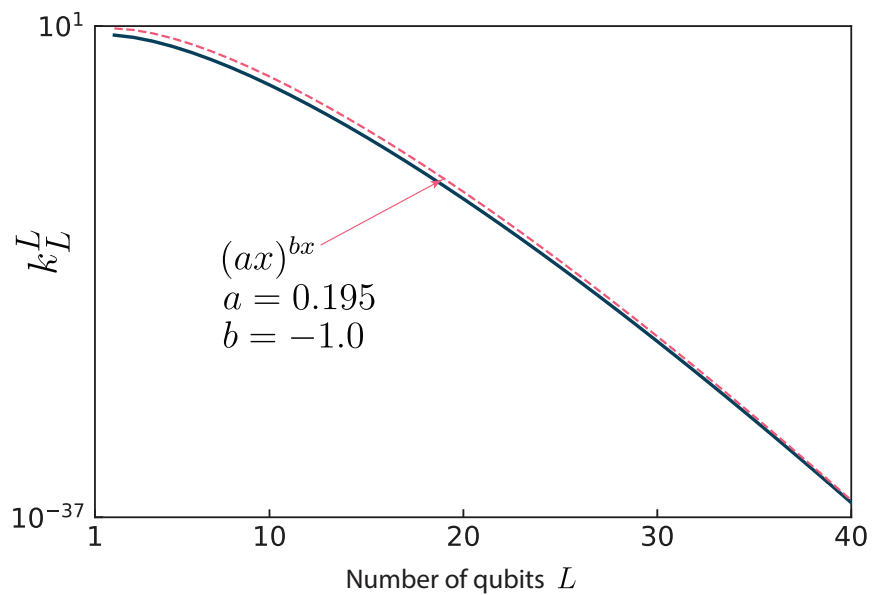


FIG. S1: The leading coefficient k_L^L in the polynomial (S18) corresponding to the equivalence class of maximal dimensionality as a function of L . The dashed line represents the superexponential fit $(ax)^{bx}$, where $a = 0.195$ and $b = -1.0$.